NSG - 668

MELLON INSTITUTE

Speculations About Plessite

T. B. Massalski, F. R. Park and L. F. Vassamillet

Summer 1965

I. INTRODUCTION

Most metallic meteorites exhibit the well-known Widmanstätten structure in which systems of parallel plates of kamacite (α, Ni-Fe), averaging a fraction of a millimeter to several millimeters in thickness, run through each large grain of the meteorite that had consisted originally of the taenite phase (γ, Ni-Fe). The resulting pattern is known as octahedral because the crystallographic planes along which kamacite segregation from taenite has occurred correspond to the original {111} family of planes of the taenite which has the multiplicity of eight. The content of Ni in the kamacite phase in different octahedrites shows considerable variation, approximately between 5.5 and 7.5% Ni. Recently some variation has also been reported in kamacite-nickel content between plates of different thickness in a single octahedrite sample.[1]

The polyhedral spaces between the kamacite plates correspond to the original fcc matrix, i.e., the taenite. In polished and etched specimens these areas show progressive stages of internal decomposition which result in dark etching effects, and such decomposed areas are generally referred to as plessite. Undecomposed original taenite can be found only near the borders of the polyhedral spaces where these are in contact with kamacite, or in exceptionally narrow bands. Plessite is highly variable in structure, grain size and composition. Other minerals that occur throughout metallic meteorites in various amounts are troilite, FeS; schreibersite, $(Fe,Ni)_3P$; cohenite, $(Fe,Ni)_3C$; and graphite. However, these minerals occur in relatively small amounts, the major constituents of a metallic meteorite being iron, nickel and cobalt ($\frac{1}{2}$%).

The general appearance of the octahedral pattern and the thickness

of individual kamacite bands depends on the angle at which the reference {111} planes meet the polished surface. Nevertheless, the average thickness of the kamacite plates in any given octahedrite tends to be a function of the total nickel content and hence octahedrites are subdivided into coarse, medium, and fine, according to previously suggested schemes.[2]

Although numerous studies of octahedrites and the Widmanstätten pattern have been made following chemical and metallographic examinations, new stimulus to the understanding of the conditions under which this pattern has formed has been provided by the use of electron probe microanalyzers whereby detailed profiles of nickel content, and other elements, across the Widmanstätten pattern can be obtained.[3-9] Such studies have shown that, whereas the percentage of nickel content in the kamacite phase remains more or less uniform, the nickel content in the undecomposed taenite in the areas immediately adjacent to kamacite phase is high, and then decreases rapidly with distance from the interface. The Ni content in the interior of decomposed taenite polyhedrons (i.e., in the plessite) is erratic because this structure usually contains a mixture of both high Ni (γ) and low Ni (α) phases. Nevertheless, it has been claimed in recent discussions[9] that an average trend in Ni content can be estimated, even on moving away from the undecomposed taenite into the decomposed areas, provided that the plessitic structure is finally divided; in cases where this has been determined, the trend continues the steady decline initiated in the undecomposed taenite phase, although less rapidly. At a point approximately equidistant from all bounding kamacite regions, Ni content usually reaches a minimum; and thus, as has been already pointed out in numerous previous publications, a linear traverse across a polished kamacite-taenite-plessite-taenite-kamacite region reveals the approximately M-shaped profile[9]

as shown diagramatically in Fig. 1.

It is now nearly universally agreed that the Widmanstätten patterns have formed in iron meteorites as they cooled from an initially homogeneous γ-iron phase into the duplex $\alpha + \gamma$ phase structure. Quite naturally the details of the structures obtained are related to the nature of the phase diagram involved, and in most cases the binary iron-nickel phase diagram is considered as an adequate basis for discussion.[8,10] The exact boundaries of the phase fields in this phase diagram are particularly difficult to determine because the reactions involved are extremely sluggish and, at low temperatures, never fully proceed to completion. For this reason various modifications of the Fe-Ni phase diagram have been proposed,[9,11,12] the most recent data concerning the portion that is associated with the formation of the Widmanstätten pattern is shown in Fig. 2. Most authors believe that the Widmanstätten pattern is formed as a result of slow cooling of the original large-grained taenite phase (γ) through the $\alpha + \gamma$ phase field, the reaction being initially an equilibrium one and becoming progressively non-equilibrium with the fall of temperature.

The process of cooling of a typical octahedrite through the two-phase field has been described in detail previously[8,9,10] and need not be repeated here. We shall only state that at any given α/γ interface nickel atoms must move by solid state diffusion into the interiors of one or both phases in order to maintain the equilibrium composition and proportions as the system cools. The kamacite plates initially form as nuclei on the crisscrossing octahedral planes of the taenite below temperatures for which the composition line crosses the $\gamma/(\gamma + \alpha)$ phase boundary and they grow in thickness with decreasing temperature, the likely rate

of decrease being of the order of 1-20°/10^6 years.[7-9] Eventually a temperature is reached at which diffusion is too sluggish to allow more nickel to reach the interiors of the remaining γ phase polyhedrons, now enriched to some 12-18% Ni. With further cooling, therefore, the distance over which equilibrium distribution of nickel can be effectively maintained in the γ phase continues to shorten with the result that the equilibrium content of nickel (i.e., high values of the order of 40-50% characteristic of low temperatures) are found only very near to taenite/kamacite boundaries. Eventually the impoverished nickel regions of the remaining taenite polyhedra are so badly out of equilibrium that they frequently undergo a separate, localized decomposition into a fine-grained mixture of equilibrium kamacite and taenite.

It is undoubtedly true that the detailed understanding of the way in which the Widmanstätten pattern has formed should permit reasonable guesses about the nature of processes that the samples containing such a pattern have undergone, i.e., the thermal history, mechanical history, etc. This in turn means that such parameters as the total time of cooling, the pressures involved, and the temperatures, have to be understood, ultimately leading also to the description of the size of the body (or bodies) from which the sample came, its constitution, and environment. The constitution, composition gradients, and the general nature of the plessite are linked with the Widmanstätten pattern. We shall concern ourselves here mainly with the question to what extent the measured composition gradients in the plessite areas can be meaningfully interpreted.

The development of the "M" profile in the taenite can be represented diagramatically as in Fig. 3. As temperature keeps falling, a depression

in the Ni content becomes pronounced in the middle of the taenite area (Fig. 3c), while the total level of the Ni content in kamacite increases slightly. Ultimately, when diffusion proceeds at a negligible rate, the profile expected resembles that shown in Fig. 3d in which, in addition to the "M" profile mentioned earlier, a border depression to slightly lower Ni contents is also observed in the kamacite. This has been detected by a number of authors[6,7,8] and most likely is associated with the reversal of the $\alpha/\alpha + \gamma$ phase boundary in the Fe-Ni phase diagram towards lower Ni content below the temperature of approximately 450°C (see Fig. 2).

Assuming that plessite results from the internal decomposition of the non-equilibrium taenite, its formation can be depicted diagramatically as in Fig. 4. Initially, rather coarse α-phase precipitation is expected to occur in the central portion of the "M" profile because the low Ni content of these areas is associated with a higher initial $\gamma \rightarrow \alpha$ transformation temperature. α-phase precipitates formed in the central portions will have opportunity to grow in size during the subsequent fall of the temperature unlike those that will form eventually in the regions of higher Ni content at progressively lower temperatures. Hence, finer and finer scale α-phase precipitation might be expected as one moves away from the central portion of a non-equilibrium taenite polyhedron. Although the individual α and γ areas in such plessitic regions might be expected to be nearly in equilibrium with respect to one another, there will be, of course, the usual differences in the Ni content between each α and γ particle as shown diagramatically in the figure. Nevertheless, provided that the scanning spot of a microprobe analyzer embraces an area greater than that of the individual particles in the plessite, an average composition trend should be obtainable from a scan; and this should reflect the gen-

eral M-shaped trend that existed in the taenite phase prior to its decomposition. Thus, although the plessitic area is no longer homogeneous, it should be possible in principle to relate the obtained M profile to cooling conditions that existed in the taenite phase prior to its decomposition, i.e., at the time when the rate-controlling factor was the diffusion of Ni in the fcc phase governed by the diffusion coefficient D_γ. On the other hand, the slight curvature observed in the border areas in the kamacite phase should be related to the diffusion of Ni in the bcc α-phase and related to the diffusion coefficient D_α. If a given cooling model, involving the pressure, temperature, and undercooling conditions of the parent meteoritic body is to be correctly interpreted, one must be able to reconstruct the M profile with the assumption that all α precipitation in the plessite has occurred in a manner suggested above.

A serious complication occurs, however, if, after the development of the M profile in the taenite, a martensitic transformation $\gamma'' \rightarrow \alpha_2''$ occurred at least in the part of the taenitic phase, resulting in the production of the non-equilibrium bcc phase which is of the same composition as that of the individual taenite region from which it has formed. The possibility of the occurrence of martensitic transformations is suggested by the experimentally determined M_s temperatures in the binary Fe-Ni alloys[13] (see Fig. 2), and also by the fact that martensitic transformation products are frequently observed in the borders of plessitic areas both in octahedrites and pallasites.[14] If the M_s temperature is sufficiently high, i.e., above ~350°C, it is then reasonable to expect the martensite to decompose subsequently into the equilibrium γ and α phases; but the process may be expected to be goverened by different diffusion rates, in agree-

ment with the fact that the decomposing martensitic phase is body-centered cubic and strained, with diffusion rates of Ni perhaps some hundred times faster than in the taenite phase of the same composition. Thus, in portions of the M profile for which the total undercooling prior to decomposition brings the possible plessitic decomposition below the M_s line, a much more complicated diffusional process is to be expected. This is illustrated in Fig. 4b in which the central portion of the M profile is depicted as "normal" plessite, the regions immediately adjoining this portion as martensite which has subsequently decomposed, and finally, the remaining regions as undecomposed martensite and border taenite with no decomposition at all. In such a situation, it may also be expected that even if martensite in the border areas (corresponding to high Ni contents and therefore low M_s temperature) did not undergo decomposition into α and γ phases, it may have undergone some localized equalization of the steep diffusion gradient, the rate-controlling process being again related to the diffusion of Ni in a strained bcc phase.

The problem in the interpretation of the diffusion profiles reconstructed from plessitic areas carries with it the following questions:

1. Has the formation of martensite been at all involved in the process, and what are the M_s temperatures of this martensite as related to the composition gradients?

2. Have such martensites decomposed fully or partially into $\alpha + \gamma$ regions by the reactions $\alpha_2 \rightarrow \alpha + \gamma$, and is there any evidence for a change in the corresponding diffusion profile reconstructed from such regions?

3. Has any equilibration (or tempering) occurred in the seemingly undecomposed martensitic areas, and

4. Are there any other more complex features in plessite that require careful interpretation?

In the following experimental work and discussion we present some evidence which at least in part answers the above questions.

II. EXPERIMENTAL PROCEDURES

Samples of the Canyon Diablo, Bristol, Bethany and Toluca meteorites were prepared for metallographic examination and microprobe analysis. Small slices mounted in a conducting resin were prepared for metallographic examination in the usual way except that after grinding through the fine abrasive papers, a flat matte surface was prepared by lapping on a lead lap wheel with 10μ carbide abrasive. This was followed by polishing with diamond to 3μ particle size followed by a brief polish on 0.3μ alumina. The sample was then etched with 5% picral or nital. After the desired areas were chosen and marked for microprobe analysis, the sample was repolished on a 3μ diamond wheel to remove the etched layer. Following microprobe analysis the sample was then photographed, cleaned by very briefly touching to a polishing wheel, etched and photographed again. The first micrograph showing the contamination marks deposited by the electron beam is then compared with the second micrograph so as to accurately relate the microprobe measurements to the microstructure. The use of the brief polishing procedure to clean the sample before etching and photographing was required because the contamination marks protected the surface during etching and hid the necessary details of the microstructure.

Simultaneous Ni and Fe concentration profiles were measured with an Applied Research Laboratories electron microprobe x-ray analyzer. Oper-

ating conditions are listed in Table I. Although both Fe and Ni were measured, only Ni concentrations are reported here. The precision of the measurements is controlled by the sensitivity and counting time. With counting time of the order of 30 seconds, the number of counts gathered in the low (5%) Ni regions was of the order of 15,000, providing a precision of approximately $3\sigma = 2.4\%$, which corresponds to 0.15 wt.% Ni.

The accuracy of the measurements was established using a series of Fe-Ni alloys prepared by Dr. G. R. Speich of the United States Steel Research Laboratories. The measured Ni concentration versus the as-cast composition is shown in Fig. 5. The deviation from linearity agrees with that expected for the Fe-Ni system.[15,16] The calculated curve is that obtained using the Ziebold-Ogilvie procedure,[17] and corresponds to an α_{AB} value of 1.06.

III. EXPERIMENTAL RESULTS

As suggested in the Introduction, the examination of dark etching plessitic areas, which under small magnification usually appear as areas of densely-precipitated duplex phases, has shown that under higher magnification several distinct regions which can be identified. For the purpose of description a typical example may be taken from the plessitic area of the Bristol meteorite shown in Fig. 6 in which successive stages of magnification reveal, on moving from the border to theinterior regions, a clear light-etching taenitic edge immediately adjoining the kamacite phase, which is followed by a narrow range of martensitic structures, and finally by a duplex mixture of both α and γ phases. Another such detailed area is shown in Fig. 7, which is taken from the Bethany meteorite. In

both cases the corresponding microprobe trace showing the trend of the nickel content is included. These two figures and Fig. 8, corresponding to another plessitic area in the Bristol meteorite, strongly suggest that the martensitic transformation has indeed been involved in the formation of plessite during the thermal history of each meteorite. In fact, some of the features suggested in the diagramatic Fig. 4b are confirmed by the experimental data. The light-etching taenitic edge is usually of the order of 5-10μ in width depending of course upon the angle of section that the polished interface makes with the plessitic polyhedron. Within such light areas the increase of Ni content is very steep and presumably corresponds to the gradient of Ni characteristic of the M profile prior to any decomposition.

There appears to be a definite change of slope in the Ni profile upon entering, or some point within, the area which corresponds to martensitic, or partly martensitic structure (see Figs. 6 and 7). Martensitic structure immediately adjoining the light-etching taenite border corresponds to about 26 wt.% Ni (see Fig. 7) which, with the use of the phase diagram shown in Fig. 2, indicates approximately a transformation in the vicinity of the room temperature. Hence, it may be concluded that even though all diffusion-controlled decomposition has ceased, the martensitic transformation proceeded in the Ni-rich portions of the M profile areas on further cooling down to room temperature. The obtained results further suggest that the discernible change in slope of the Ni content in the martensitic areas may be correlated with Ni content falling slightly below 20 wt.% down to about 17 wt.%. This therefore suggests that some diffusion-controlled adjustment of the composition gradient has occurred

in these areas at temperatures in the region of 200 to 300°C, again assuming the validity of the diagram shown in Fig. 2. Martensite, which has formed above those temperatures, i.e., in the range of 300-600°C, appears to have undergone in most cases a major decomposition into near equilibrium $\alpha + \gamma$ mixtures. This is evident metallographically in all three figures. In such areas the contours of the α and γ precipitation appear to follow the general directions of a prior martensitic decomposition so that a distinct directionality is observed. However, judging by the fine-grained structure of the α phase, the grain boundary pattern, and the distinct appearance of the γ phase grains, there seems to be no doubt that the observed structure is a decomposition structure of a prior martensitic area and not a singular kamacite precipitation from a single phase polyhedron of the γ phase as would be expected by a "normal" plessitic process described in the Introduction. That there has been greatly enhanced diffusional activity during the martensite decomposition is emphasized by the appearance of a distinct rim composed of Ni-rich taenite particles such as that marked R in Fig. 7, which can be identified both in the photomicrographs and in the microprobe traverses. The generation of this rim appears to be connected with the rejection of Ni out of the martensite plates and into the newly-precipitating γ phase located in the region between martensite plates until the residual α_2 phase attains the equilibrium concentration value of Ni. This situation is particularly well illustrated in the Bethany meteorite where a layer of enhanced γ precipitation is distinctly visible. In the Bristol meteorite (Fig. 8) the range of Ni-rich γ precipitation immediately adjoining the martensitic region is again quite clear. It may be noted in this figure that both α and

γ particles within the decomposed area have the typical polycrystalline duplex structure.

We conclude therefore, at least on the basis of the presented evidence, that in the majority of cases where the Ni concentration in the M profile has never risen above approximately 25%, martensitic decomposition has occurred and was followed by decomposition into $\alpha + \gamma$ structures. The distinct γ rim observed in the microstructures falls approximately in the region corresponding to about 15 (or less) wt.% Ni along the original M profile; and this suggests that a further diffusional decomposition occurred in all martensitic structures that formed above approximately 300°C. Thus, in the majority of octahedrite structures whose over-all composition falls in the range between 8 and 13 wt.% Ni, martensite transformation may be presumed to have interferred with the normal plessitic decomposition. In most such cases initial super-cooling and build-up of Ni in the border areas prevented a diffusional decomposition above ~600°C. The above conclusions are of course based on the use of the presently-known Fe-Ni phase diagram established at 1 atmosphere of pressure.

A few additional features are of interest. During the high temperature formation of the Widmanstätten pattern some remaining γ regions become sufficiently narrow at high temperatures to enable them to maintain a substantially high Ni content even in the central region during the fall of temperature. An example of this is shown in Fig. 9 taken from Canyon Diablo meteorite. Here the bottom of the M curve falls above some 27 wt.% Ni and consequently, apart from some etching effect, no distinct decomposition or change in the trend of Ni content is observable. It may be presumed that such areas will yield the typical M profile of

Ni content whose distribution is governed primarily by the diffusion of Ni in the taenite phase. They can thus be used for a successful reconstruction of the cooling process. Goldstein and Ogilvie[11] have indeed recently determined the times and temperatures governing the conditions of cooling of meteorite bodies using specimens of such relatively high Ni content (Carlton - 12.77 wt.% Ni and Dayton - 18.10 wt.% Ni). If plessitic areas containing evidence of a martensite decomposition were to be used for the same purpose, only the rims free of any decomposition would correspond to the original M profile developed in the taenite, and their width is probably insufficient for an accurate analysis.

Finally, a rather coarse decomposition area corresponding to what may be presumed a normal high-temperature plessitic decomposition is shown in Fig. 10, taken from the Toluca meteorite. Here the average Ni content of the α particles does vary with their width as suggested by Goldstein[1], and the typical borderline depression in the kamacite phase marked A in the figure may be seen not only where the whole plessitic area borders on the kamacite, but also at the borders of individual α particles. It appears that for some reason this border depression is somewhat lower inside the plessitic areas than at the boundaries of the taenite and kamacite. The reason for this could be two-fold: either an evidence of enhanced diffusion as a result of strain during the growth of α particles at relatively low temperatures or, as suggested by Goldstein,[1] this is directly related to the width of the kamacite particle and it is further evidence of the reverse of the $\alpha/\alpha + \gamma$ boundary at temperatures below some 400°C.

CONCLUSIONS

We conclude that in the majority of cases where plessite is exam-

ined in detail there are indications that its formation is intimately related to the formation of martensite during the cooling history. The composition of the borderline martensite-free regions indicate that martensitic decomposition has been taking place down to room temperature as may be expected for a martensitic process, while the decomposition of martensite into a duplex $\alpha + \gamma$ structure terminated approximately above 300°C and was followed only by very localized adjustments of composition in the remaining martensite. The area of a major martensitic decomposition into two phases is separated from the area of a more restricted diffusional activity by a rim of γ precipitation or a Ni-enriched phase as evidenced by microprobe traverses. We conclude that only the portions of an M profile which show no decomposition of any kind are suitable for a careful mathematical analysis and interpretation leading to the time-cooling conditions in the parent meteorite bodies. These conclusions are speculative to the extent that too few samples have been studied to prove the generality of the above arguments. It is our feeling that a more critical approach to the choice of samples and sample regions for detailed study is advised. Of particular importance appears to be the necessary correlation between microstructure and microprobe traces.

Acknowledgments

The authors are grateful for stimulating discussions held at various times with Drs. Goldstein, Ogilvie and Frederickson. The assistance of Mr. T. Rohrer with experimental work is acknowledged.

This work has been supported by a grant from the National Aeronautics and Space Administration, Washington, D.C.

References

1. Goldstein, J. I., NASA Report #X-641-65-205 (1965).
2. See, for example, Massalski, T. B. in Researches on Meteorites. A Symposium, edited by C. B. Moore, p. 107, J. Wiley & Sons, New York (1962).
3. Yavnel', A. A., Borovski, I. B., Ilin, N. P. and Marchukova, I. D., Doklady Akad. Nauk. SSSR, 123, 256 (1958).
4. Maringer, R. E., Richard, N. A. and Austin, A. E., Trans. AIME, 215, 56 (1959).
5. Feller-Kniepmeyer, M. and Uhlig, H. H., Geochim. et Cosmochim. Acta, 21, 257 (1961).
6. Agrell, S. O., Long, J. V. P. and Ogilvie, R. E., Nature, 198, 749 (1963).
7. Short, J. M. and Andersen, C. A., J. Geophys. Res., in press (1965).
8. Goldstein, J. I. and Ogilvie, R. E., Geochim. et Cosmochim. Acta, in press (1965).
9. Wood, J. A., Icarus, 3, 429 (1964).
10. Massalski, T. B. and Park, F. R., Journal of Geophysical Res., 67, 2925 (1962).
11. Goldstein, J. I. and Ogilvie, R. E., submitted to Trans. Met. Soc., AIME (1965).
12. Rao, M. and Winchell, P., private communication.
13. Kaufman, L. and Cohen, M., Trans. AIME, 206, 1393 (1956).
14. Massalski, T. B. and Park, F. R., Geochim. et Cosmochim. Acta, 28, 1165 (1964).
15. Birks, L. S. and Seebold, R. E., Anal. Chem., 33, 687 (1961).
16. Goldstein, J. I., Hanneman, R. E. and Ogilvie, R. E., Trans. AIME, in press (1965).
17. Ziebold, T. O. and Ogilvie, R. E., Anal. Chem., 36, 322 (1964).

Figure Captions

1. Typical M-profile of Ni concentration across a kamacite-taenite-plessite-taenite-kamacite region

2. Fe-Ni phase diagram, Fe-rich portion

3. Schematic representation of the development of the "M" profile

4. Schematic representation of plessite formation
   a. nucleation and growth process
   b. martensite decomposition process

5. Calibration curve for Ni in Fe-Ni
   a. K/C vs C plot to determine α_{AB}, where K is the intensity normalized to the pure element (Ni) and C is the concentration
   b. K vs C plot

6. Bristol meteorite
   a. Photomicrographs of the structure traversed in microprobe examination at different magnifications
   b. Ni concentration vs distance along line defined by hardnes marks shown in micrograph. Insert correlates structure with composition

7. Bethany meteorite
   a. and b. Low and medium magnification photomicrographs of the area traversed in microprobe examination
   c. High magnification photomicrograph of same region with Ni concentration profile superimposed

8. Bristol meteorite of relatively coarse structure
   a. Photomicrographs at low, medium and high magnification of the structure traversed by the microprobe
   b. Ni concentration profile taken along line defined by microhardness marks and arrows

9. Canyon Diablo meteorites
   a. Photomicrographs at low and medium magnification
   b. Ni concentration profile taken along line as indicated on micrograph

10. Toluca meteorite containing coarse α particles in a γ matrix. Ni concentration profile shown below micrograph

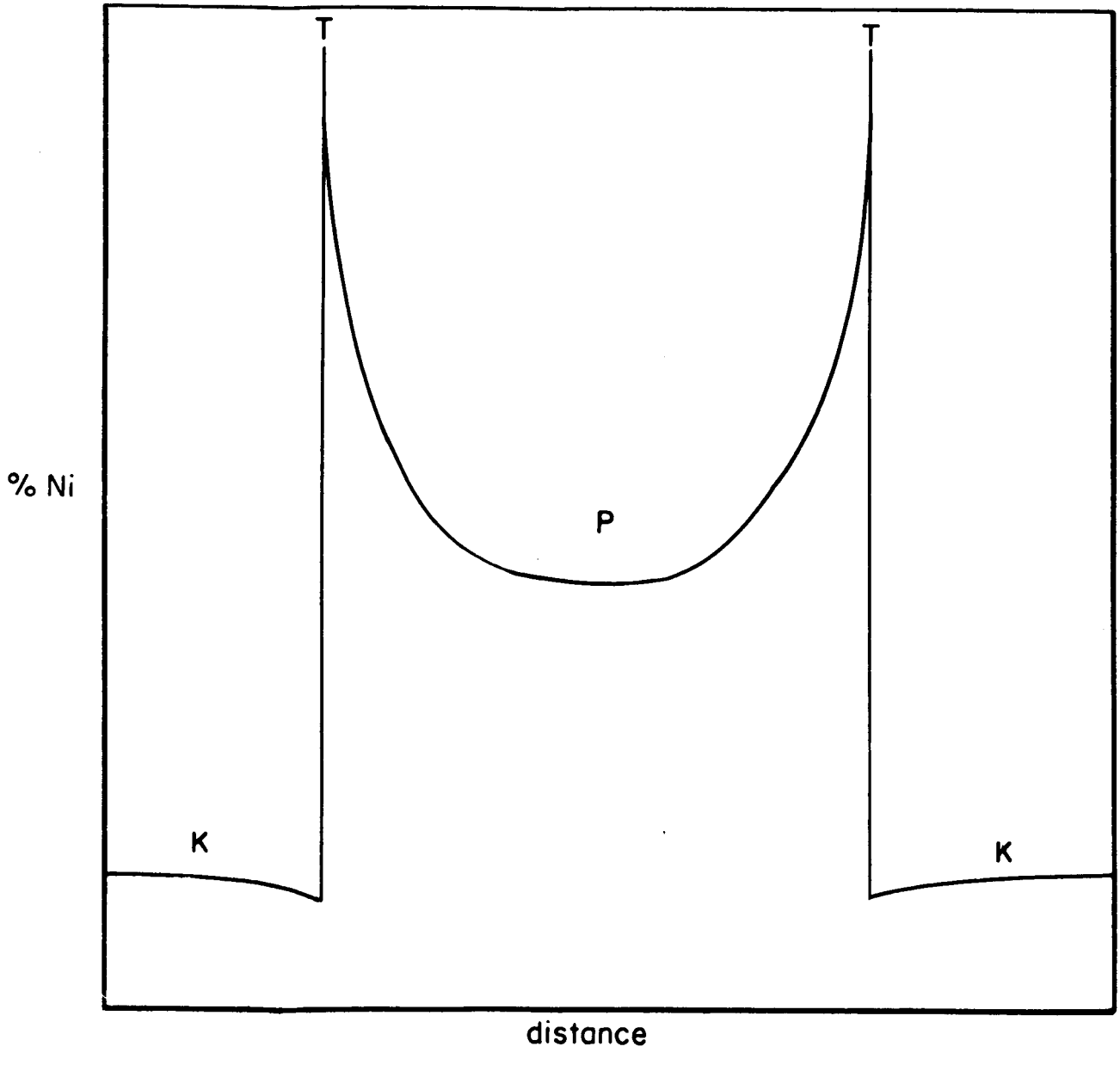

Fig 1

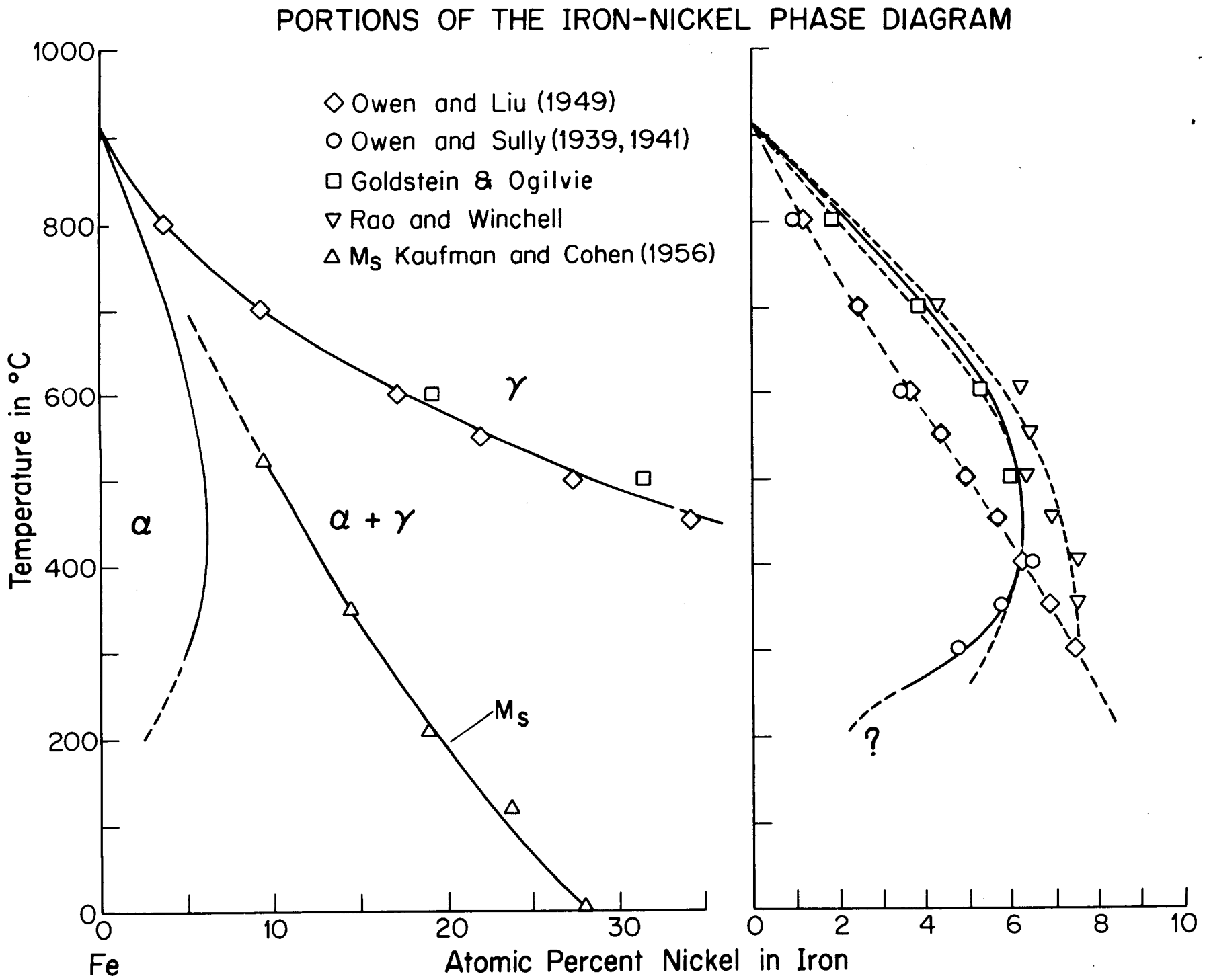
PORTIONS OF THE IRON-NICKEL PHASE DIAGRAM
Owen and Liu (1949)
Owen and Sully (1939, 1941)
Goldstein & Ogilvie
Rao and Winchell
Ms Kaufman and Cohen (1956)
γ
α
α + γ
Ms
?
Temperature in °C
1000
800
600
400
200
0
0
10
20
30
Fe
0
2
4
6
8
10
Atomic Percent Nickel in Iron

Fig. 2

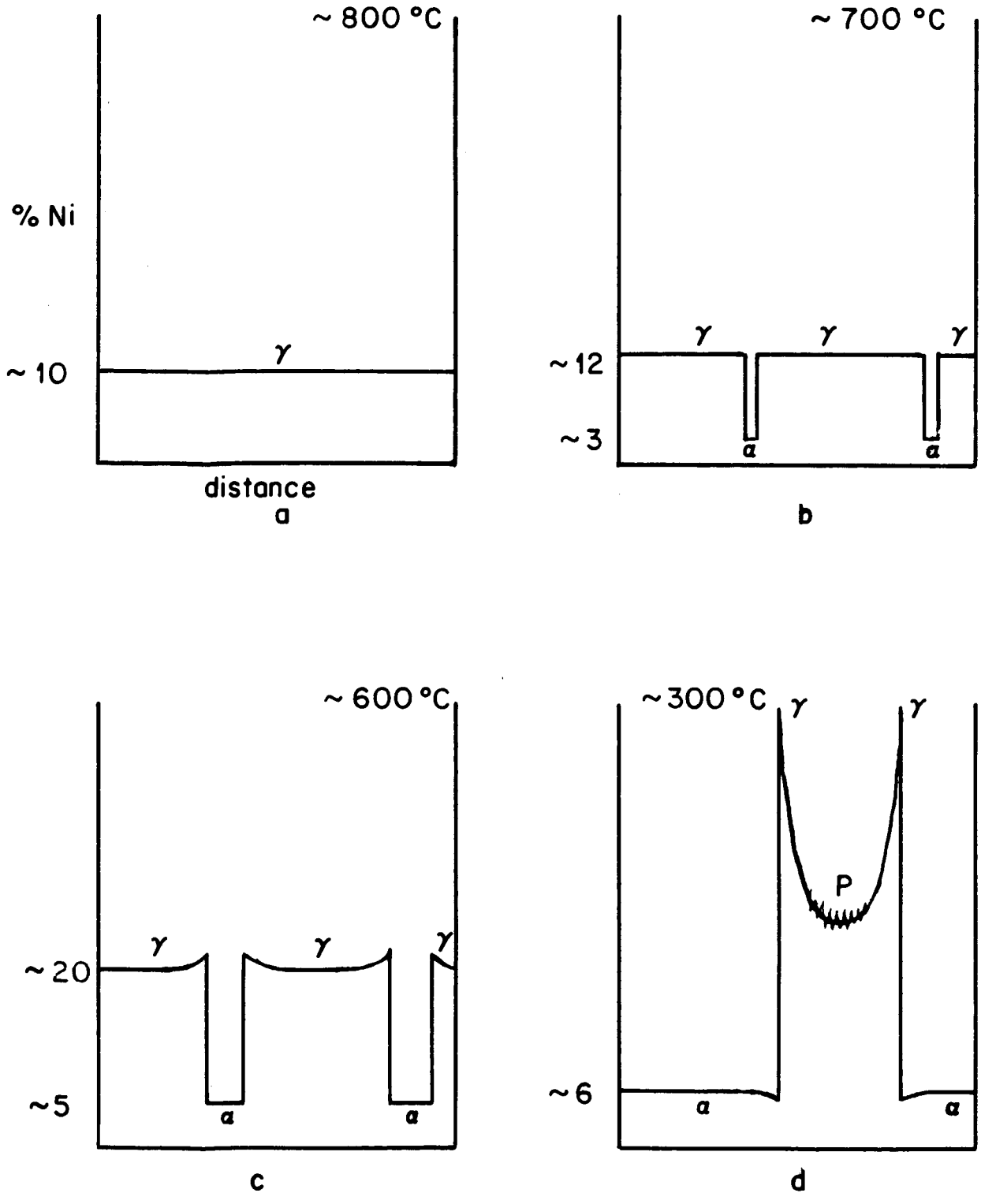
~ 800 °C
% Ni
~ 10
γ
distance
a
~ 700 °C
γ
γ
γ
~ 12
~ 3
α
α
b
~ 600 °C
γ
γ
γ
~ 20
~5
α
α
c
~ 300 °C
γ
γ
P
~ 6
α
α
d

Fig. 3

Fig. 4a

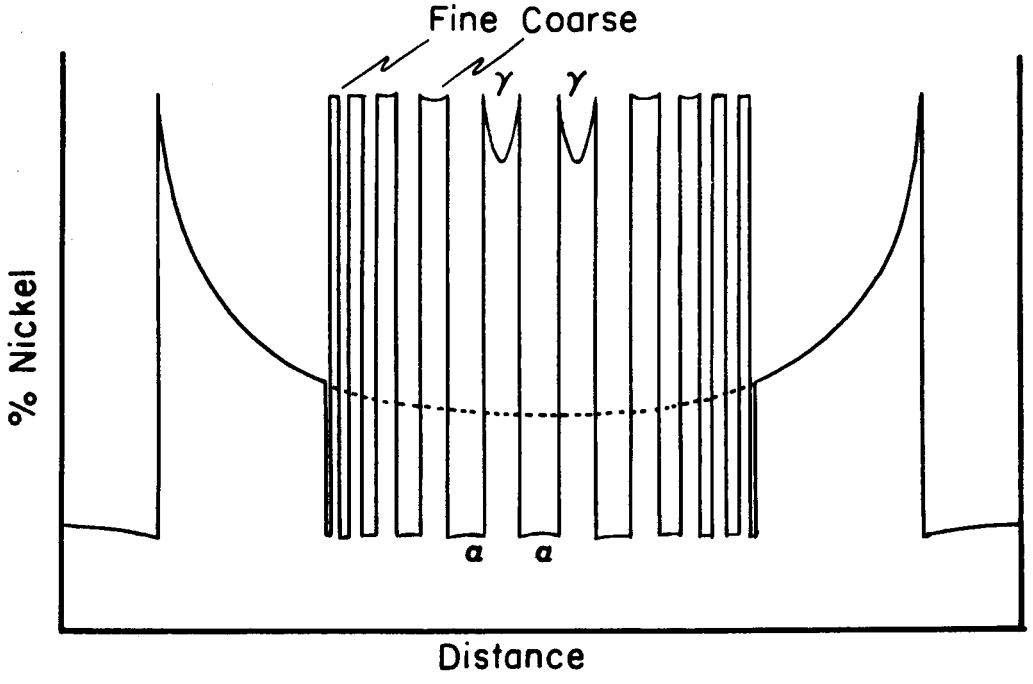
Fine
Coarse
γ
γ
α
α
% Nickel
Distance

Fig. 4b

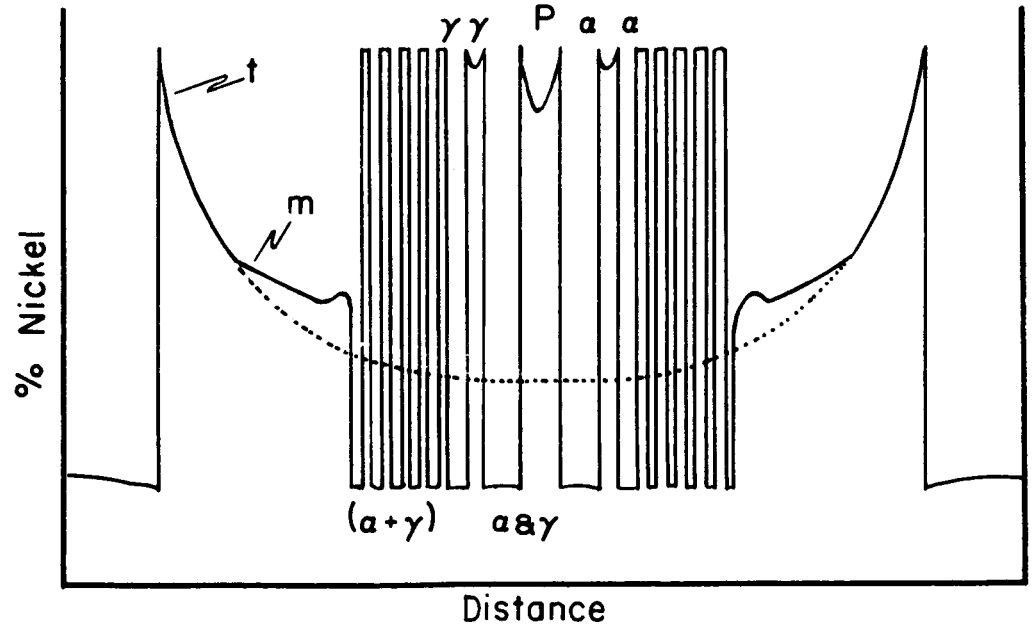
γ γ
P
α α
t
m
(α+γ)
α&γ
% Nickel
Distance

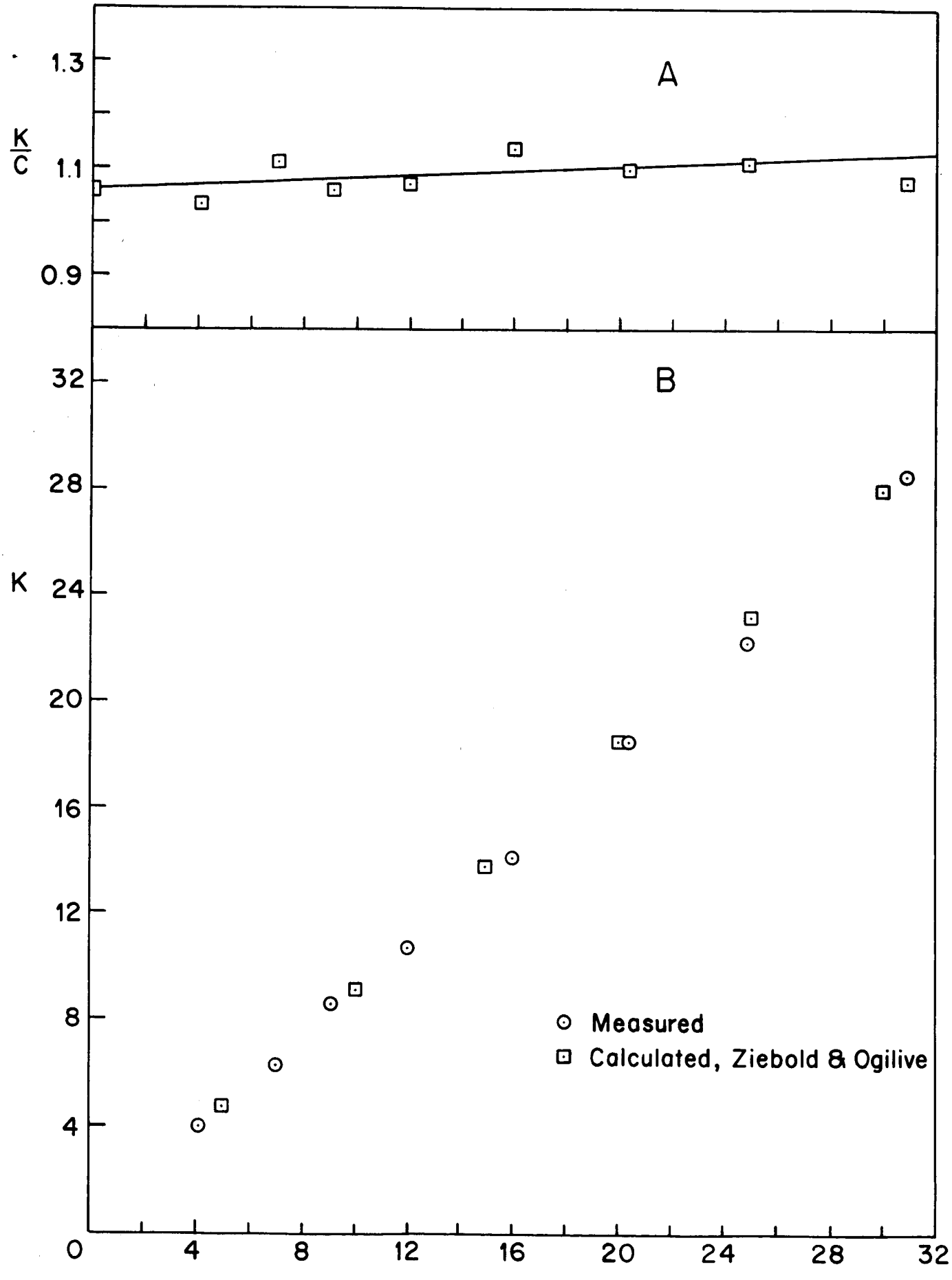
A
B
K/C
K
1.3
1.1
0.9
32
28
24
20
16
12
8
4
0
4
8
12
16
20
24
28
32
Measured
Calculated, Ziebold & Ogilive
Weight Fraction Ni (C)

Figure 5

Fig. 6

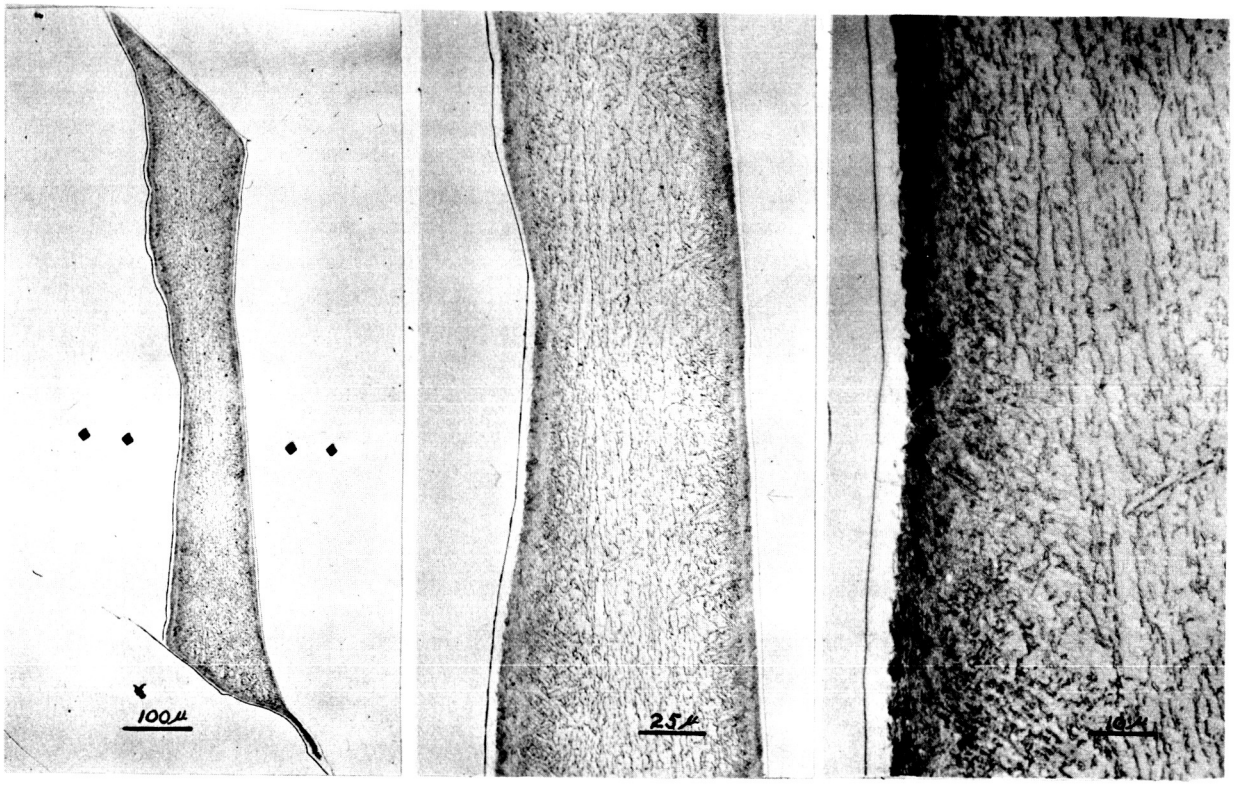
100μ
25μ

a b c

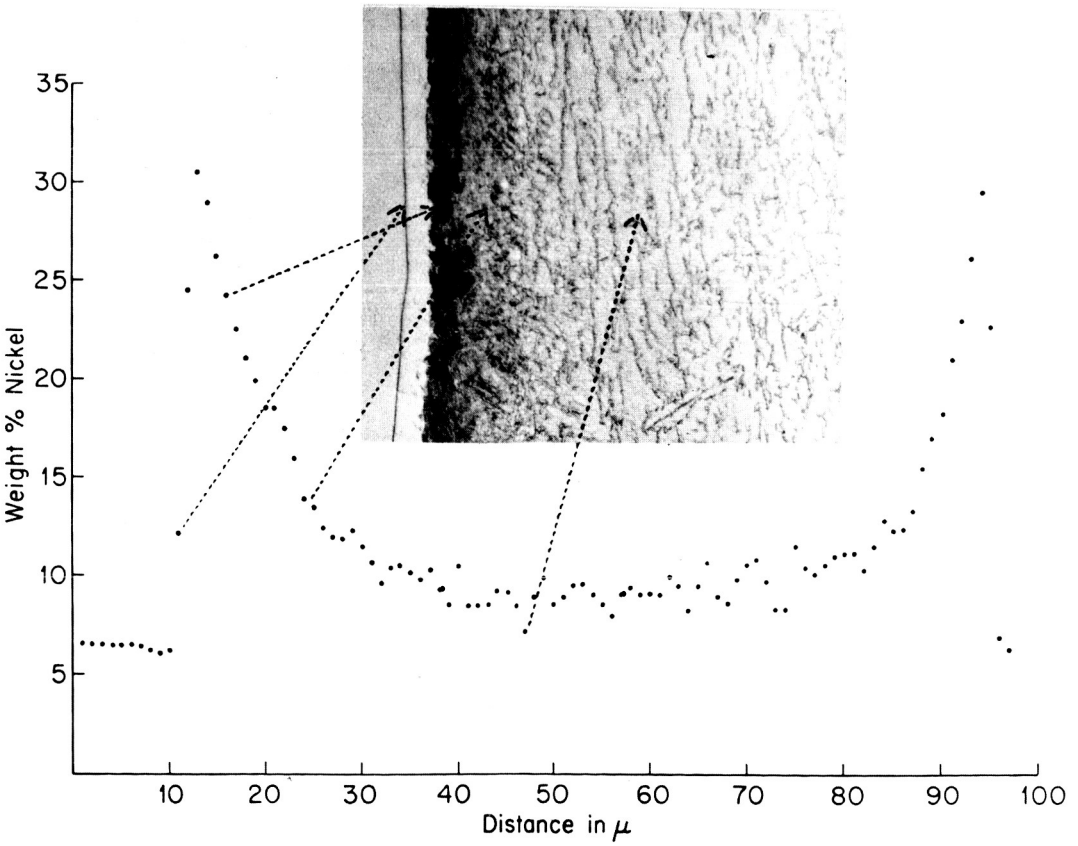
Weight % Nickel
35
30
25
20
15
10
5
10
20
30
40
50
60
70
80
90
100
Distance in μ

d

Fig 7

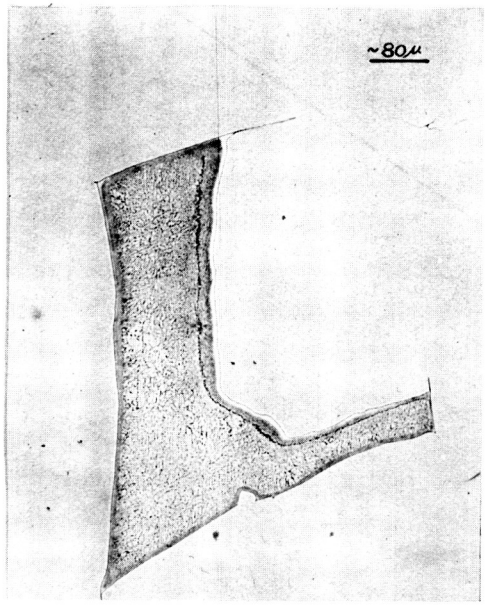

a

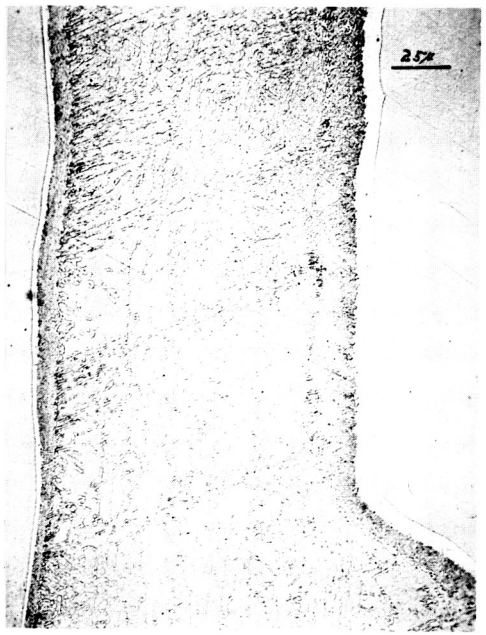

b

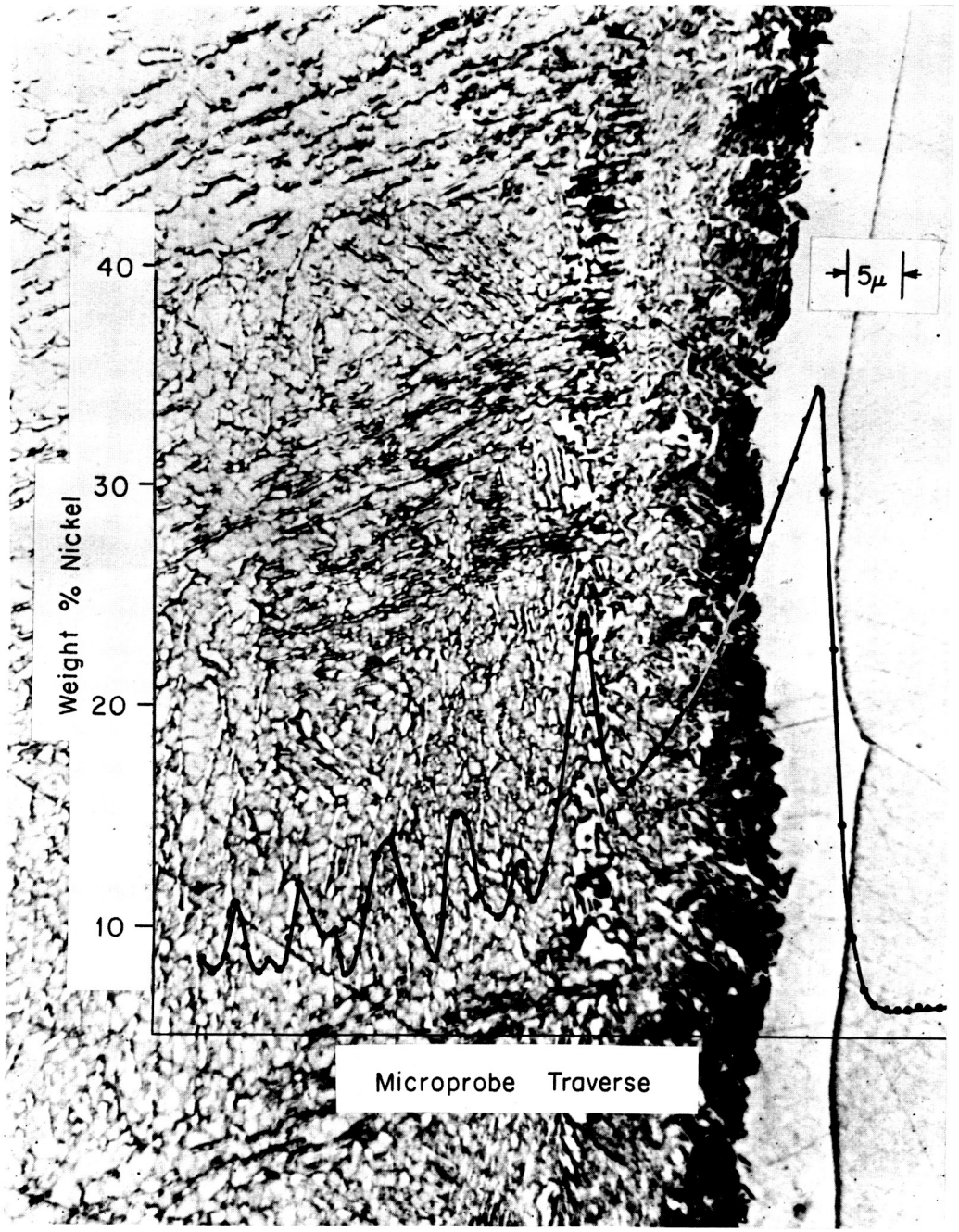

c

Fig 8

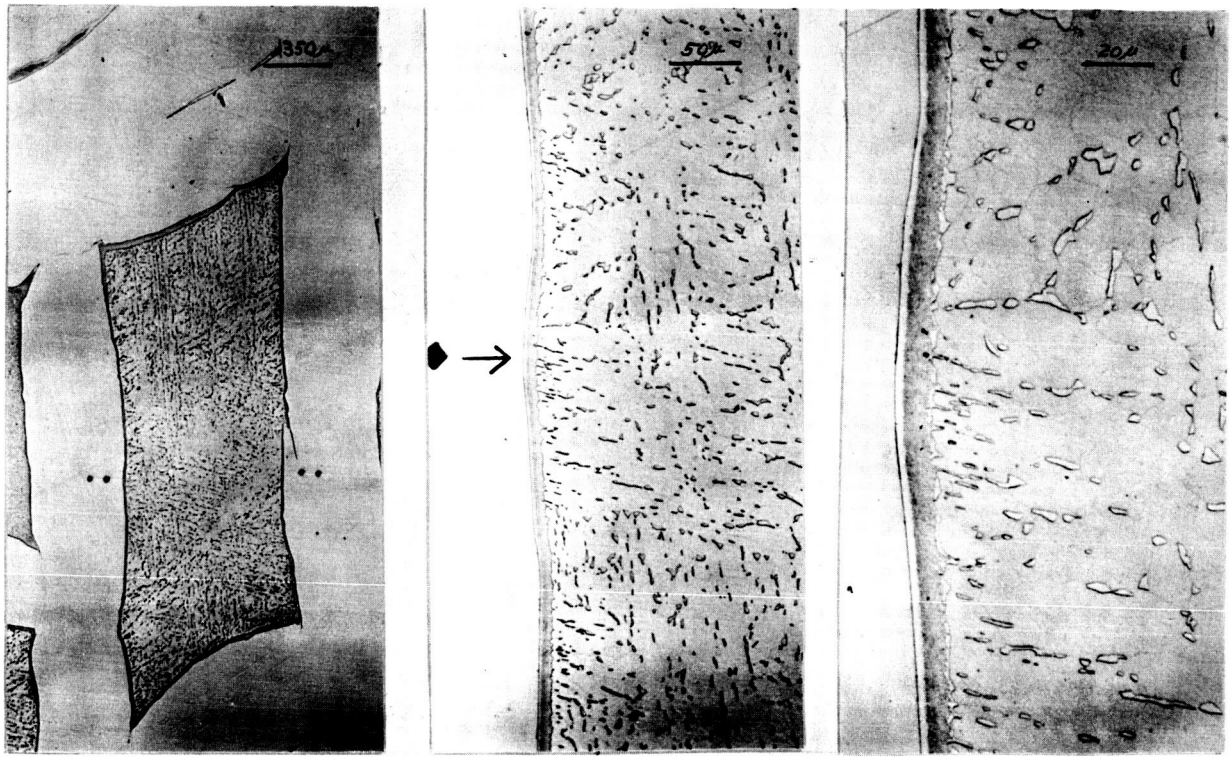
1350μ
50μ
20μ

a

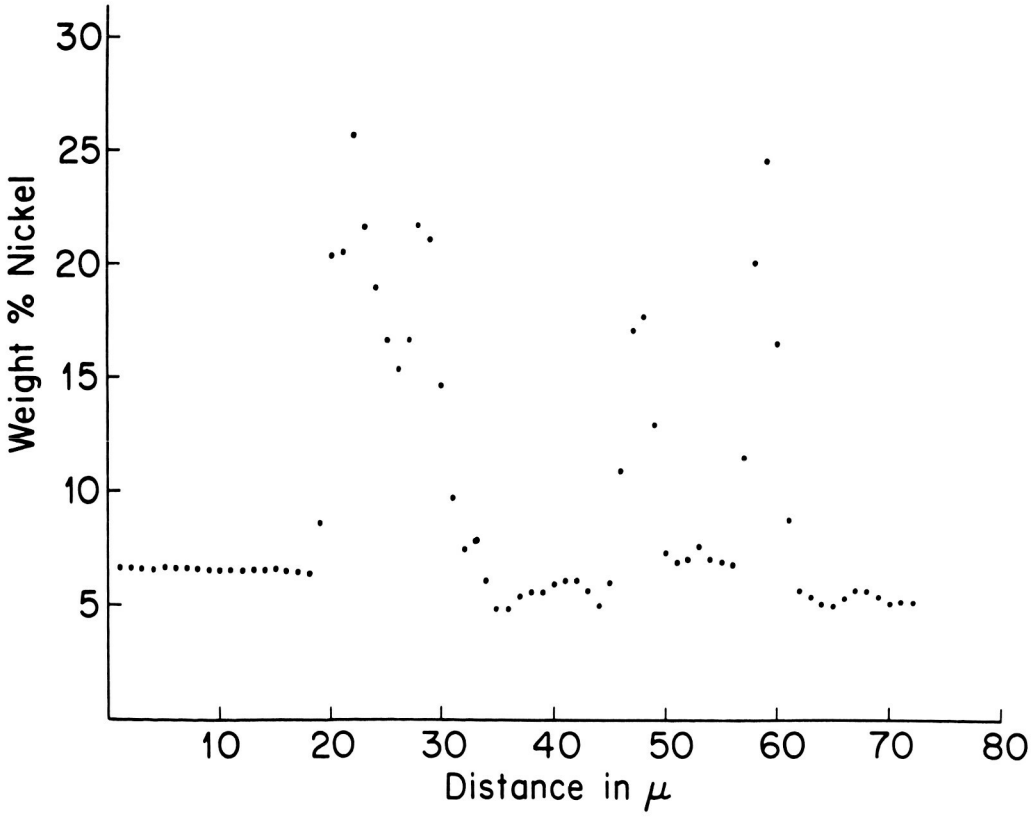
Weight % Nickel
30
25
20
15
10
5
10
20
30
40
50
60
70
80
Distance in μ

b

Fig. 9

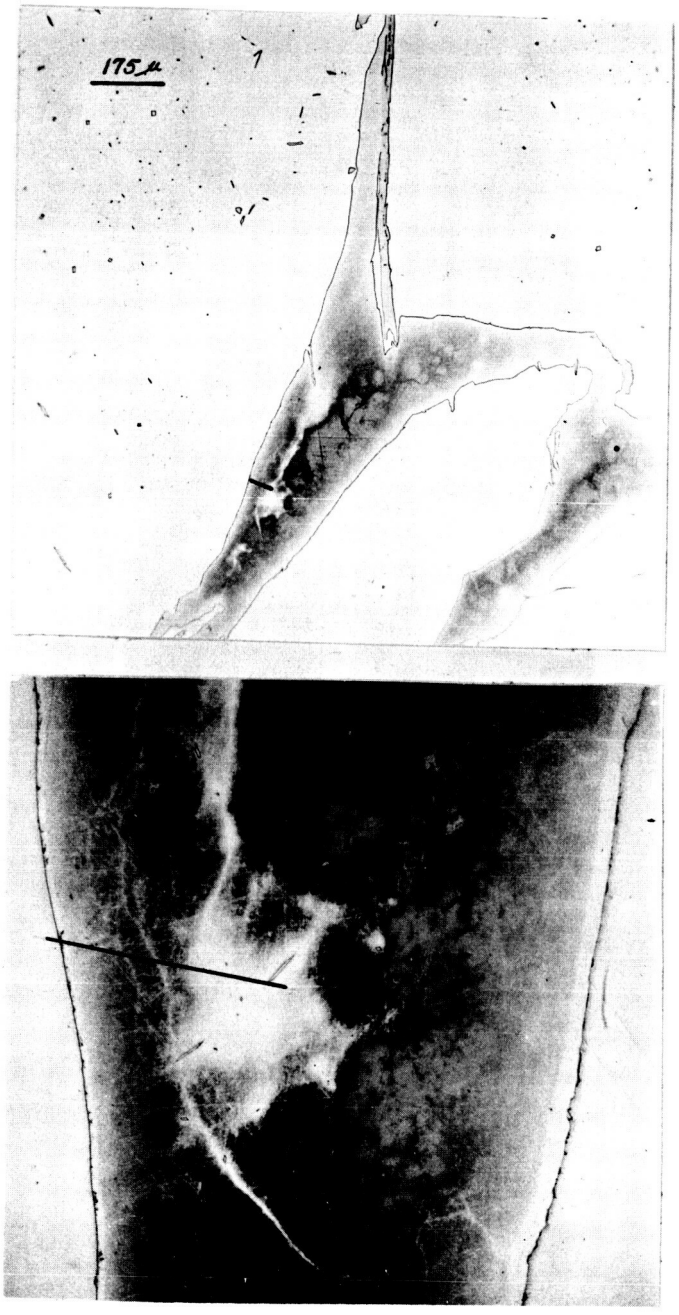

a

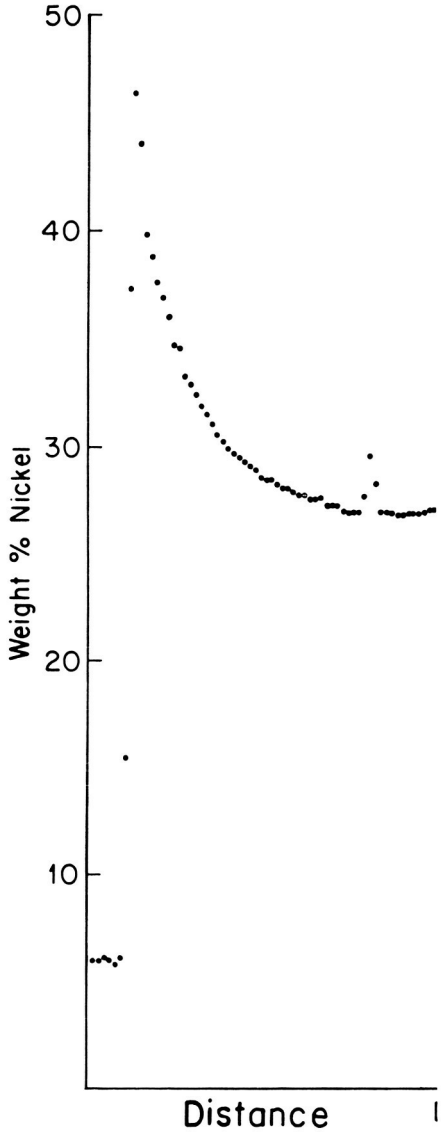

b

Fig 10

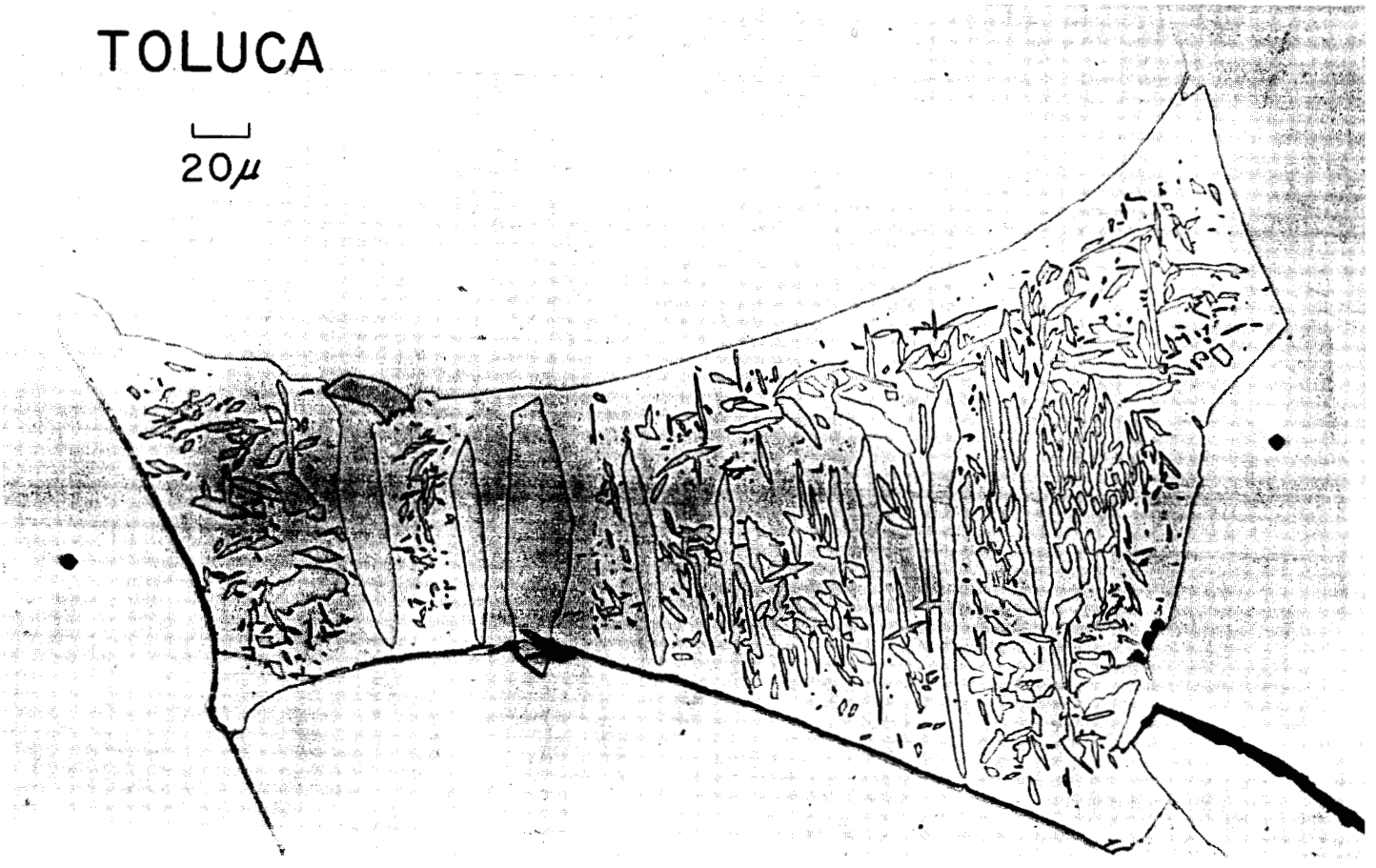

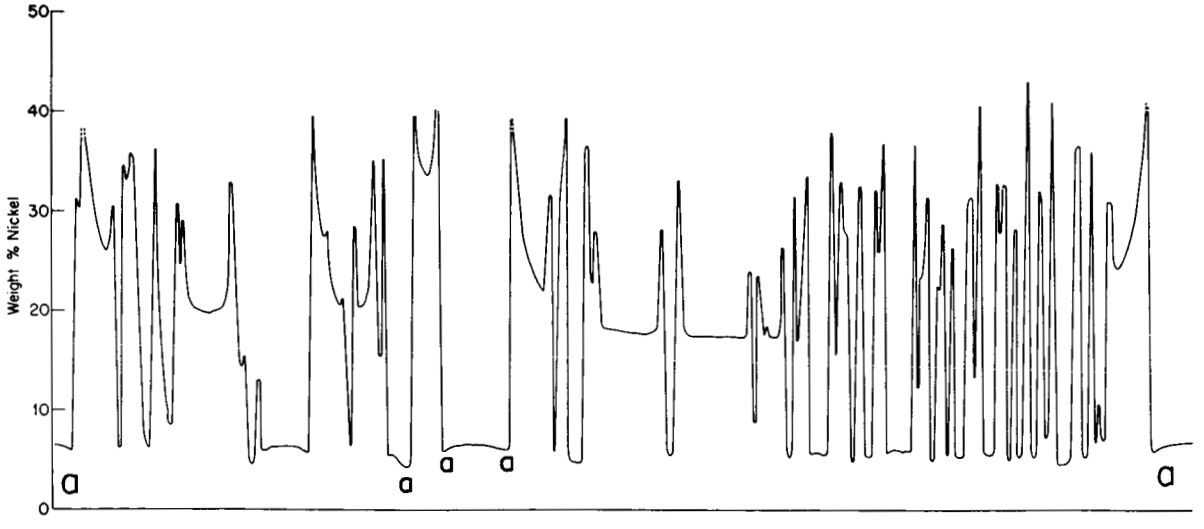

TABLE I

Accelerating Voltage	20 Kv	Sample Current .03μn
Radiation	Analyzing Crystal	Sensitivity
Ni K_α I	4" LiF	3×10^5 counts/sec-μa
Fe K_α II	4" ADP	10^5 counts/sec-μa